Prediction of the load carrying capacity of slender cross-section members under eccentric axial load. Part 1: the approach

Predizione della capacità portante di elementi con sezioni snelle soggetti ad azione assiale eccentrica. Parte 1: il metodo

Claudio Bernuzzi, Paolo Rugarli

The use of thin walled cold formed steel members as structural elements has become increasingly widespread over the last few decades. Due to the imperfections and high slenderness values found in plate elements (walls) making up members, column and beam-column performance is generally influenced by local buckling, which in many cases can interact with the stability of the overall members. This complex interaction is not taken into consideration directly in the most recent design standards, which in many case leads to a conservative assessment of the load carrying capacity of the members. This paper presents a procedure for predicting the load carrying capacity of thin walled cold-formed members under eccentric axial load. Both local and overall buckling phenomena can be taken into account by defining a suitable cross-section which is effectively resistant. The extensive validation phase is presented in the companion paper.

L'uso di membrature in acciaio formate a freddo in parete sottile è cresciuto continuamente negli ultimi decenni. A causa della contemporanea presenza sia di imperfezioni che di valori elevati di snellezza nei piatti che compongono le membrature, la risposta degli elementi presso-inflessi è generalmente influenzata dall'instabilità locale, che in molti casi può interagire con l'instabilità globale. Questa complessa interazione non è direttamente considerata nelle più recenti normative, così da portare, in molti casi, a valutazioni conservative della capacità portante delle membrature. Questo articolo presenta una procedura per predire la capacità portante di membrature formate a freddo in parete sottile in presenza di azione assiale eccentrica. E' possibile tenere contemporaneamente conto dei fenomeni sia di instabilità locale sia di instabilità globale, definendo un'opportuna sezione resistente efficace. E' stata condotta una fase di estesa validazione che è presentata in un successivo lavoro.

Keywords: cold-formed, thin-walled, effective section, axial load, resistance, local buckling, global buckling, load carrying capacity, design rules.

1. INTRODUCTION

Thin-walled cold-formed steel components for structural applications are generally formed by cold rolling of strips or coils and represent an important and growing area in the field of constructional steelwork. Their major usages are for sheetings (roof decks and curtain wall panels) as well as for beams, columns, and beam-columns, which can form complete light steel construction for housing and for other low-rise structures [1,2].

Due to the presence of thin plate elements in cold-formed profiles (i.e., high value of the ratio between the width of the section walls and their thickness), these members are generally subjected to local buckling phenomena, especially for low values of the overall slenderness. An accurate analysis of the member response is usually very complex, due to the important role played by material plasticity and imperfections. For practical design, the approaches proposed in major recent codes [3-5] for cold-formed members are based on the "effective width" concept. The regions of a plate element adjacent to supported edges are considered to be effective in carrying loads while the ones far from supported edges are considered completely ineffective in resisting compression (fig. 1). This concept was initially introduced by von Karman [6], which defined the effective width, b_e, as:

$$b_e = \left(\sqrt{\frac{\sigma_{cr}}{f_y}}\right) \cdot b \equiv \frac{b}{\bar{\lambda}_p} \equiv \rho \cdot b \leq b \qquad 1)$$

where b is the plate width, fy is the yield stress of the material, σ_{cr} represents the critical elastic buckling stress and ρ is the reduction factor.

In 1946, Winter [7] modified this expression in order to take into

account also geometrical imperfections and proposed to estimate b_e as:

$$b_e = \left[\sqrt{\frac{\sigma_{cr}}{f_y}}\left(1-0.22\cdot\sqrt{\frac{\sigma_{cr}}{f_y}}\right)\right]\cdot b = \rho\cdot b \le b \qquad 2)$$

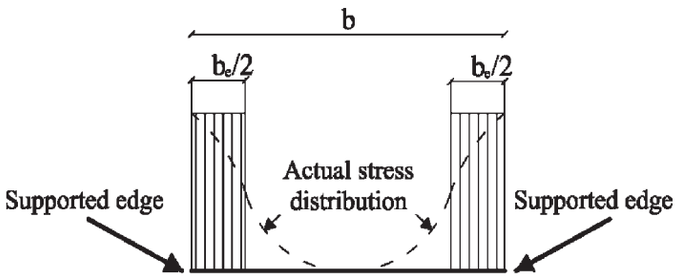

Figure 1: effective width for compressed stiffened element

It should be noted that the updated *Eurocode 3: part 1-3* [4] uses an effective width based on the rules reported in *Eurocode 3: part 1-5* [8]. In particular, the stress ratio ψ has been explicitly introduced. It is defined in accordance with the indications reported in figures 2 and 3, which are related to internal and outstand compression elements, respectively.

• For internal compression elements, the effective width is evaluated as:

$$b_e = \left\{\sqrt{\frac{\sigma_{cr}}{f_y}}\cdot\left[1-0.055(3+\psi)\cdot\sqrt{\frac{\sigma_{cr}}{f_y}}\right]\right\}\cdot b = \rho\cdot b \qquad 3a)$$

• For outstand compression elements, the effective width is evaluated as:

$$b_e = \left[\sqrt{\frac{\sigma_{cr}}{f_y}}\cdot\left(1-0.188\cdot\sqrt{\frac{\sigma_{cr}}{f_y}}\right)\right]\cdot b = \rho\cdot b \qquad 3b)$$

The critical elastic buckling stress, σ_{cr}, is evaluated as:

$$\sigma_{cr} = k_\sigma\cdot\frac{\pi^2 E}{12(1-\upsilon^2)}\cdot\left(\frac{t}{b}\right)^2 \qquad 4)$$

where E and υ are respectively the Young modulus and the Poisson's ratio of the material, k_σ is the buckling factor depending on the stress ratio ψ as well as on the boundary conditions (figs. 2 and 3), and t is the material thickness.

According to Eurocode 3 part 1-3, three different effective cross sections have to be taken into account: the first one is related to the axial force N; the second one is related to bending moment M_x; the third one is related to bending moment M_y, where subcripts x and y are related to gross section principal axes, no matter the fact that effective section principal axes are generally different, that is shifted and rotated. Each of the three effective cross sections is computed by assuming that associated internal action is amplified to reach the gross-section elastic limit, thus at least one side of the section reaches yield stress in compression. It should be noted that this approach can result in many cases to be extremely conservative. The effective resistant cross-section is also the same for very slender members, when failure is due to overall buckling which can occur owing to level of stresses too low to activate local buckling.

This paper describes an original approach to predict the load carrying capacity of thin-walled cold-formed members under constant axial load as well as constant axial load and bending moments. Since the target values are experimental data, no material safety factor gM has been used. Load carrying capacity of members is directly assessed by considering the interaction between local and overall buckling. It is obtained defining an effective cross-section which depends strictly on the value of the loads applied to members, and it is hence directly associated with the values of the stresses acting on each plate element defining member cross section. Furthermore, some examples are proposed to present key features of the method, while the degree of accuracy of the present approach can be assessed in the companion paper [9]. Finally, hand calculations are proposed in the appendix to show how the method works.

2. THE PROPOSED METHOD

The method predicts the load carrying capacity of straight members under constant axial load and constant bending moments. Under these conditions a constant effective cross section is expected along member axis.

Effective area assessment, by changing section, does change flexural and torsional properties, and this, in turn, affects the buckling behaviour of a member. Effective area computation and global buckling behaviour strictly depend on each other. As a consequence, the proposed method treats these phenomena together.

The method is based on the following assumptions:

• a straight member under a set of externally applied loads $S=(N, M_x, M_y)$ is analysed to search for the load multiplier α_R that leads the member to achieve its load carrying capacity;

• effective area computation depends on both stress distributions and stress levels on each element defining member cross-section. These stress levels and distributions are obtained from gross-section properties;

• linear stress distributions over a side are described by a stress ratio $\psi = \sigma_2/\sigma_1$ (figs. 2 and 3), where σ_1 is the maximum compressive stress over the side, assuming compression positive;

• decreasing the stress level at equal distribution, that is at equal ψ, increases effective width of the element. This effect is obtained by reducing element slenderness ($\bar{\lambda}_{p,red}$) by the following rule, taken directly from Eurocode 3: 1-3 [3]:

$$\bar{\lambda}_{p,red} = \bar{\lambda}_p\sqrt{\frac{\sigma_1}{f_y}} = \sqrt{\frac{\sigma_1}{\sigma_{cr}}} \qquad 5)$$

Stress distribution (compression positive)	Effective width b_{eff}
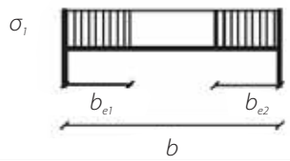	$\psi = 1$ $b_{eff} = \rho \cdot b$ $b_{e1} = 0.5 \cdot b_{eff}$ $b_{e2} = 0.5 \cdot b_{eff}$
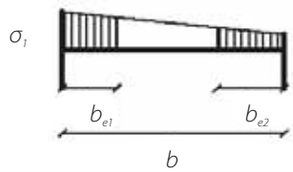	$1 > \psi \geq 0$ $b_{eff} = \rho \cdot b$ $b_{e1} = \frac{2}{5-\psi} b_{eff}$ $b_{e2} = b_{eff} - b_{e1}$
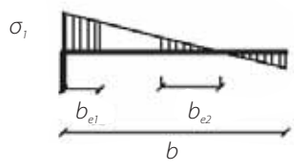	$\psi < 0$ $b_{eff} = \rho \cdot b_e = \frac{\rho \cdot b}{1-\psi}$ $b_{e1} = 0.4 \cdot b_{eff}$ $b_{e2} = 0.6 \cdot b_{e1}$

$\psi = \sigma_2 / \sigma_1$	1	$1 > \psi > 0$	0	$0 > \psi > -1$	-1	$-1 > \psi > -3$
Buckling factor k_σ	4	$\frac{8.2}{1.05+\psi}$	7.81	$7.81 - 6.29\psi + 9.78\psi^2$	23.9	$5.98(1-\psi)^2$

Figure 2: effective width for internal compression elements (from table 4.1 of [8])

Stress distribution (compression positive)	Effective width b_{eff}
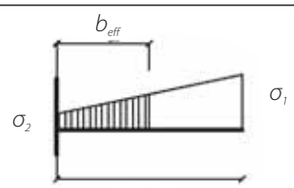	$1 > \psi \geq 0$ $b_{eff} = \rho \cdot c$
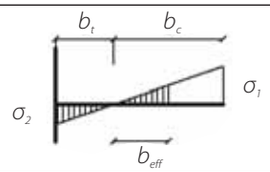	$\psi < 0$ $b_{eff} = \rho \cdot b_c = \frac{\rho \cdot c}{1-\psi}$

$\psi = \sigma_2 / \sigma_1$	1	0	-1	$-1 > \psi > -3$
Buckling factor k_σ	0.43	0.57	0.85	$0.57 - 0.21\psi + 0.07\psi^2$

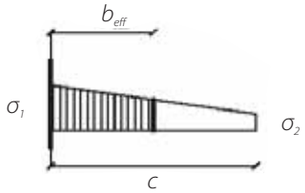	$1 > \psi \geq 0$ $b_{eff} = \rho \cdot c$
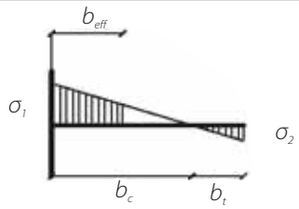	$\psi < 0$ $b_{eff} = \rho \cdot b_c = \frac{\rho \cdot c}{1-\psi}$

$\psi = \sigma_2 / \sigma_1$	1	$1 > \psi > 0$	0	$0 > \psi > -1$	-1
Buckling factor k_σ	0.43	$\frac{0.578}{\psi+0.34}$	1.7	$1.7 - 5\psi + 17.1\psi^2$	23.8

Figure 3: effective width for outstand compression elements (from table 4.2 of [8])

in which σ_1 (which is called σ_{com} in Eurocode) is the computed maximum compressive stress over the element, while $\bar{\lambda}_p$ is defined as

$$\sqrt{\frac{f_y}{\sigma_{cr}}}\ .$$

In other words, if the peak compressive stress σ_1 on the element is the yield stress for the element, the effective width will be estimated via eqs. 3a) and 3b). If, on the other hand, the peak compressive stress σ_1 is lower than f_y, then the reduction is lower and can be computed using $(\bar{\lambda}_{p,red})$.

• flexural and torsional buckling loads of a partially effective member are computed using merely effective section properties, that is neglecting ineffective element parts. Gross-section properties are used for buckling checks only if the section is fully effective;

• a unique effective section Ω_e is associated with a load multiplier α of a set of externally applied loads S. The corresponding effective cross section properties are used to evaluate a global multiplier α^*, related to member load carrying capacity by means of a suitable interaction formula. This term α^* is generally different from the original α used to determine effective section Ω_e;

• it is assumed that the correct load multiplier α leads to an effective-section member, the load carrying capacity $\alpha^* S$ of which is exactly equal to αS, therefore $\alpha=\alpha^*$ is the condition searched for. This condition is usually achieved by means of an iterative procedure.

In computing effective member load multiplier α^*, the shift of the centroid of the section must be taken into account (fig. 4), which generates additional bending moments, and, also, the rotation of principal axes of effective section from the original principal axes of the member gross-section. The first effect transforms pure tension or pure compression into tension plus bending or compression plus bending. The second effect transforms a simple monoaxial bending into a biaxial bending.

Therefore the standard load condition over effective section is actually the more general one, that is, axial load plus biaxial bending.

In detail, the method can be summarized in seven key steps, in accordance with the flow chart presented in figure 5, as described below:

Step 1. - initialization of load multiplier α with an upper bound α_1, which is estimated by using the gross-section linearized plastic limit domain. Set $i=1$;

Step 2. - stress computation for gross section elements under load level $\alpha_i S$ and assessment of related effective widths;

Step 3. - effective section properties computation (let $\Omega_{e,i}$ be the effective section, identifying the effective member);

Step 4. - transforming applied loads to the effective section reference system, $\alpha_i S_{e,i}$, as a function of $\alpha_i S$ and of geometrical properties;

Step 5. - evaluation of multiplier α_i^* which brings the effective member to its load carrying capacity $\alpha_i^* S_{e,i}$;

Step 6. - evaluation of error measure and check for tolerance;

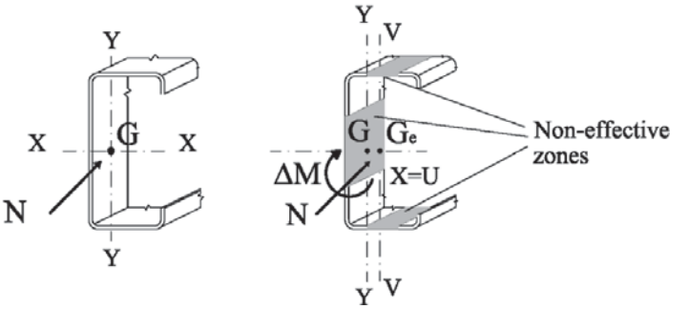

Figure 4: gross and effective cross-section: shift of centroidal axis

Step 7. - correction and new iteration. If error is lower than tolerance, then stop; otherwise go back to step 2 using α_{i+1} and setting $i=i+1$.

In the following sub-sections, more details on each of these seven steps are reported.

2.1 INITIALIZATION OF LOAD MULTIPLIER α WITH AN UPPER BOUND α_1 ESTIMATED USING GROSS-SECTION LINEARIZED PLASTIC LIMIT DOMAIN

Gross-section linearized plastic limit domain is used to evaluate an upper bound to the member capacity. The equation considered to

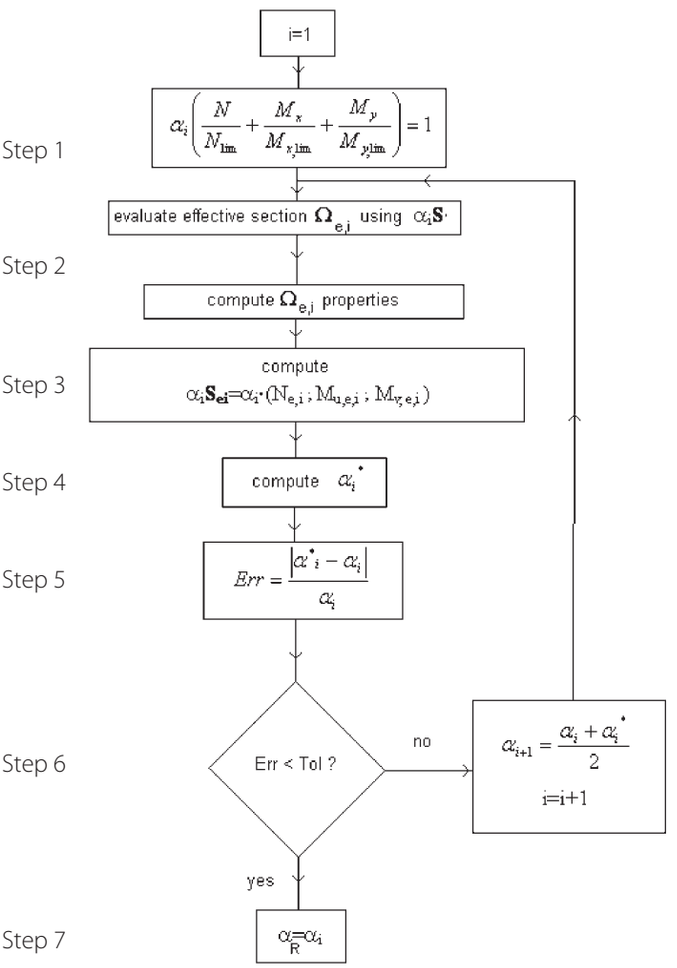

Figure 5: flow-chart of the proposed method

obtain the load multiplier α_1 related to the first iteration is:

$$\alpha_1\left(\frac{N}{N_{lim}}+\frac{M_x}{M_{x,lim}}+\frac{M_y}{M_{y,lim}}\right)=1 \qquad 6)$$

where subscripts "*x*" and "*y*" are related to the principal axes of the gross-section, while subscript "lim" indicates the limit value of axial (*N*) or bending (*M*) resistance.

In the first iteration, axial and bending resistances are evaluated by considering gross-section properties in terms of area (A_g) and section plastic moduli ($W_{g,x,pl}$ and $W_{g,y,pl}$), i.e. $N_{lim}=A_g f_y$, $M_{x,lim}=W_{g,x,pl} f_y$ and $M_{y,lim}=W_{g,y,pl} f_y$.

2.2 STRESS COMPUTATION AND ASSESSMENT OF EFFECTIVE WIDTHS

The stress distribution is computed over straight elements, while curved elements are considered fully effective. Using gross-section properties, the stress $\sigma(P)$ at a generic point $P(X,Y)$ is given by:

$$\sigma(P)=\frac{\alpha_i N}{A_g}+\frac{\alpha_i M_x}{I_{g,x}}Y-\frac{\alpha_i M_y}{I_{g,y}}X \qquad 7)$$

Hence, the computation of the stresses at the extremes of any straight element is immediate.

Let σ_1 and σ_2 be the stresses at the element extremes. Using well established methods, such as the procedure proposed in Eurocode 3 (figs 2 and 3) the effective widths of each straight element can be computed.

The set of all fully effective elements (curved elements and fully effective straight elements) together with effective parts of partially effective straight elements, defines the effective section Ω_e. Since the effective section changes from iteration to iteration, it will be identified by symbol $\Omega_{e,i}$. The effective section defines a set of new elements, generally unconnected one to each other due to the presence of ineffective parts.

Although from iteration to iteration the resistance moduli used to compute stresses are always those of the gross-section (i.e. $W_{g,x}$ and $W_{g,y}$), since the load level changes – via α_i - also the effective section $\Omega_{e,i}$ does change, being effective widths not only a function of stress distribution but of stress intensity as well, via $\overline{\lambda}_{p,red}$.

2.3 COMPUTATION OF EFFECTIVE SECTION PROPERTIES

Effective properties are computed in a straightforward manner as a sum of the contributions of each element belonging to the effective section $\Omega_{e,i}$. No simplification of section by removing curved sides has been used, since curved elements contributions to the computation of centroid position, area, second area moment, section elastic moduli, are evaluated exactly by means of closed-form formulae [10,11].

A new centroid $G_{e,i}$ is evaluated, which is not generally coincident with the original one, *G*, of gross-section, and $(X_{e,i};Y_{e,i})$ are the coordinates of $G_{e,i}$ with respect to the gross-section principal axes (fig. 6). New principal axes of the effective section, named u_i and v_i, are in general rotated through an angle φ_i from the original gross-section principal axes (*X, Y*).

The warping constant of the effective section, in general made up of unconnected sides, has been computed in accordance with the thin-walled open-section torsion theory. The effective section can be seen as the assembly of internally connected open sections, each of which behaves as in open section theory (Vlasov's). Thus, it has been assumed that the warping constant is determined by using the same rules valid for connected open sections, simply as the integral sum of the effective side contributions.

2.4 COMPUTATION OF LOADS APPLIED TO THE EFFECTIVE SECTION

The externally applied load $\alpha_i S$ to the member gross-section has to be considered acting on the effective section. As a consequence, axial force $\alpha_i N$ has to be shifted from *G* to $G_{e,i}$, hence generating bending moments $\alpha_i \Delta M_{x,i}$ and $\alpha_i \Delta M_{y,i}$ in addition to the existing $\alpha_i M_x$ and $\alpha_i M_y$. Neglecting for the sake of simplicity the presence of the load multiplier α_i, it can be seen that:

$$\Delta M_{x,i} = -NY_{e,i} \qquad 8a)$$
$$\Delta M_{y,i} = NX_{e,i} \qquad 8b)$$

where *N* is assumed positive if tensile.

The total bending moments $M_{x,i,T}$ and $M_{y,i,T}$ referred to the gross-section principal axes (*X,Y*) are thus:

$$M_{x,i,T} = M_x - NY_{e,i} \qquad 9a)$$
$$M_{y,i,T} = M_y + NX_{e,i} \qquad 9b)$$

Finally, the rotation of the effective section's principal axes (u_i,v_i) can be taken into account leading to the values of bending moments $M_{u,e,i}$, $M_{v,e,i}$ defined as:

$$M_{u,e,i} = M_{x,T,i}\cos(\varphi_i) + M_{y,T,i}\sin(\varphi_i) \qquad 10a)$$
$$M_{v,e,i} = -M_{x,T,i}\sin(\varphi_i) + M_{y,T,i}\cos(\varphi_i) \qquad 10b)$$

By considering now the load multiplier α_i, the direct transformation from $\alpha_i S$ to $\alpha_i S_{e,i}$, that is, from the gross-section axes to the effective section axes, leads to the following expressions of the loads applied to the effective section:

$$\alpha_i N_{e,i} = \alpha_i N \qquad 11a)$$
$$\alpha_i M_{u,e,i} = \alpha_i (M_x - NY_{e,i})\cos(\varphi_i) + \alpha_i (M_y + NX_{e,i})\sin(\varphi_i) \qquad 11b)$$
$$\alpha_i M_{v,e,i} = -\alpha_i (M_x - NY_{e,i})\sin(\varphi_i) + \alpha_i (M_y + NX_{e,i})\cos(\varphi_i) \qquad 11c)$$

2.5 EVALUATION OF THE MULTIPLIER α_i* CORRESPONDING TO THE EFFECTIVE MEMBER LOAD CARRYING CAPACITY α_i*$S_{e,i}$

On the basis of effective section properties, as well as of the values of the load on the effective section, the load multiplier associated with the achievement of member capacity can now be estimated. In the present approach, this is done by using interaction formulae, keeping into account both axial load and bending moments.

In the present work the interaction formulae presented in the following sub-sections have been used.

2.5.1 TENSION FORMULA

A linearized elastic limit domain has been assumed, which yields the limit multiplier α_i* as:

$$\alpha_i^* = \frac{1}{\left(\frac{N}{N_{e,i,lim}} + \frac{|M_{u,e,i}|}{M_{u,e,i,lim}} + \frac{|M_{v,e,i}|}{M_{v,e,i,lim}} \right)} \qquad 12)$$

where $N_{e,i,lim}=A_{e,ify}$, $M_{u,e,i,lim}=W_{u,e,i} f_y$ and $M_{v,e,i,lim}=W_{v,e,i} f_y$.

2.5.2 COMPRESSION FORMULA

The case of a member under a compressive axial load is here considered, and the interaction formula which has been used is given by:

$$\frac{\alpha_i^* |N|}{N_{e,i,lim}} + \frac{\alpha_i^* |M_{u,e,i}|}{M_{u,e,i,lim}(1-\frac{\alpha_i^* |N|}{N_{cr,u,e,i}})} + \frac{\alpha_i^* |M_{v,e,i}|}{M_{v,e,i,lim}(1-\frac{\alpha_i^* |N|}{N_{cr,v,e,i}})} = 1 \qquad 13)$$

It should be noted that this equation, which is well known and has been used for decades, has been chosen due to its simplicity. Current approaches recommended by recent codes are based on more refined rules, which have not been herein considered, being out of the scope of the present research.

The interaction formula proposed by eq. 13) leads to a third order equation, which can be written as:

$$a(\alpha_i)^3 + b(\alpha_i)^2 + c(\alpha_i) + d = 0 \qquad 14)$$

where constant terms a, b, c and d are expressed as:

$$a = |N|^3 M_{u,e,i,lim} M_{v,e,i,lim} \qquad 15a)$$

$$b = -|N|^2 M_{u,e,i,lim} M_{v,e,i,lim}(N_{e,i,lim} + N_{cr,u,e,i} + N_{cr,v,e,i}) - |N| N_{e,i,lim}(M_{u,e,i} N_{cr,u,e,i} M_{v,e,i,lim} + M_{v,e,i} N_{cr,v,e,i} M_{u,e,i,lim}) \qquad 15b)$$

$$c = |N| M_{u,e,i,lim} M_{v,e,i,lim}(N_{cr,u,e,i} N_{cr,v,e,i} + N_{e,i,lim} N_{cr,u,e,i} + N_{e,i,lim} N_{cr,v,e,i}) + + N_{e,i,lim} N_{cr,u,e,i} N_{cr,v,e,i}(|M_{u,e,i}| M_{v,e,i,lim} + |M_{v,e,i}| M_{u,e,i,lim}) \qquad 15c)$$

$$d = -N_{e,i,lim} M_{u,e,i,lim} M_{v,e,i,lim} N_{cr,u,e,i} N_{cr,v,e,i} \qquad 15d)$$

The lowest positive real root of eq. 13) defines the load multiplier α_i*. Terms in eq. 15) are explained below:

• flexural buckling critical loads ($N_{cr,u,e,i}$ and $N_{cr,v,e,i}$) are computed in a standard way, referring to the effective section's principal axes. Effective length factors β_u and β_v have to be determined in the current effective section's principal axes, being defined in the input data phase in the original gross-section principal axes reference system (β_x, β_y). The problem is here solved by assuming an elliptic transition formula, depending on angle φ_i so that terms β_u and β_v can be evaluated simply as:

$$\beta_u = \beta_x \cos^2(\varphi_i) + \beta_y \sin^2(\varphi_i) \qquad 16a)$$

$$\beta_v = \beta_x \sin^2(\varphi_i) + \beta_y \cos^2(\varphi_i) \qquad 16b)$$

• $N_{e,i,lim}$ is computed using Eurocode 3 buckling curves [3,4]. This way of computing $N_{e,i,lim}$ only takes into account flexural buckling ($N_{e,i,limF}$). More generally $N_{e,i,lim}$ has been taken as the minimum between the flexural buckling load and the flexural-torsional buckling load ($N_{e,i,limFT}$).Therefore:

$$N_{e,i,lim} = min\{N_{e,i,limF}, N_{e,i,limFT}\} \qquad 17)$$

• bending moment limits $M_{u,e,i,lim}$ and $M_{v,e,i,lim}$, are computed as in the tension-side equation, that is: $M_{u,e,i,lim}=W_{u,e,i} f_y$ and $M_{v,e,i,lim}=W_{v,e,i} f_y$, being $W_{u,e,i}$ and $W_{v,e,i}$ the elastic bending moduli computed over the current effective section and referring to the effective section's principal axes.

2.6 CHECK FOR TOLERANCE

Once the load multiplier α_i* has been computed, it is necessary to estimate an error value and, if needed, a new iterative value for α. In particular, if the original α_i results too high, effective parts are too small, and the computed α_i* will be lower than α_i. On the other hand, if α_i is too low, effective parts are too large, and the computed α_i* will be too high.

As an error measure, the following error index has been used:

$$Err_i = \frac{|\alpha^*_i - \alpha_i|}{\alpha_i} \qquad 18)$$

The value of tolerance "*tol*" must be defined for an acceptable error limit, i.e. if $Err_i < tol$, then $\alpha_R=\alpha_i$. Otherwise, a new estimate for α and a new iteration is needed. It has to be noted that assuming *tol=0.001* it is possible to obtain results characterized by a more than satisfactory degree of accuracy with a quite limited number of iterations.

2.7 CORRECTION AND NEW ITERATION

If $Err_i > tol$, a new iteration is needed. New value of the load multiplier has to be defined in the correction phase. In the present

study, the new load multiplier is calculated:

$$\alpha_{i+1} = \frac{\alpha_i + \alpha_i^*}{2} \qquad 19)$$

Once the new value of the load multiplier is defined, the procedure requires to jump to step 2 assigning $i = i+1$.

3 THE SOFTWARE PROGRAMME

The algorithm described in section 2 has been developed into an existing component of the 3D finite element program Sargon©[11], produced and developed by the software house Castalia s.r.l.. This program was yet able to manage very general thin-walled sections, computing automatically elastic and plastic properties of gross-sections also by means of boundary integrals, as explained in [10]. This feature enables the computing of cross sections having both straight and curved sides in a very general way, including the computation of plastic moduli. Moreover, the program is capable of considering sections with holes inside and also of graphically rendering section drawings. These features allowed a relatively easy implementation of the algorithm developed and presented in this paper, and a relatively simple test and control phase, which, otherwise, would have been quite long and complex. The algorithm was written as a new method of the existing general C++ class "COLD", which is implemented into the DLL "SHAPES.dll" of Sargon©.

Each computation was started using a unit axial load. Thus, the final load multiplier a is exactly the load carrying capacity estimate for the applied axial load N. A value of 0.001 has been considered as tolerance limit (i.e., tol=0.001) to stop the iterative procedure.

4 APPROACH APPLICATIONS

As previously mentioned, this approach has been validated by considering the state-of-the-art of tests on thin-walled members. In the companion paper [9] the prediction of the load-carrying capacity of 229 specimens experimentally tested is presented, to allow a direct appraisal of the degree of accuracy of the unified approach. In the following, six of these cases have been considered and main data associated with the iterative procedure are presented, in order to allow a better understanding of key features of the proposed method. In particular, two types of cross-section are herein considered:

- angle cross-section (fig. 7a);
- lipped channel cross-section (fig. 7b).

For each cross section, three specimens with different value of the effective length (and hence, of different overall slendernesses) have been considered. Material as well as geometrical data necessary to define members are deduced from papers [12,14], where tests have been described.

In tables 1 and 2, related respectively to angles and channels, the data listed below are presented for the first, for an intermediate

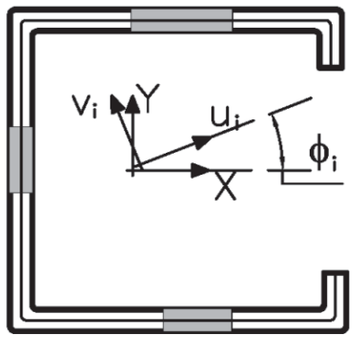

Figure 6: shift of centroid and principal axis from gross to effective section

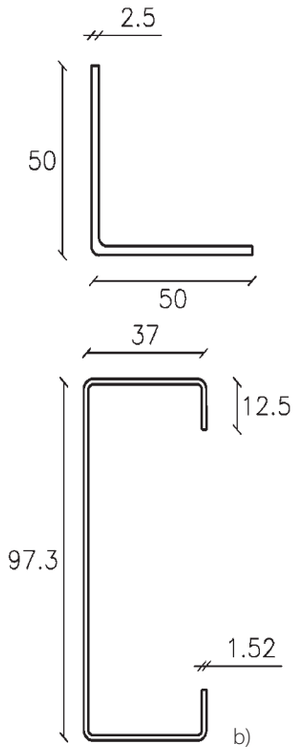

Figure 7: gross-section of angle (a) and lipped channel (b) specimens considered in examples

and for the last iteration:

- the value of the load multiplier α_i at the beginning of the i^{th} iteration;
- the value of the form factor Q_i defined as the ratio between the effective area, $A_{e,i}$, and the gross area A_g (i.e., $Q_i = \frac{A_{e,i}}{A_g}$);
- the values of the effective second moment of area, $I_{e,u,i}$ and $I_{e,v,i}$, in the principal axis of the effective section. It has to be pointed out that all the 229 cases considered in the validation phase are related to mono-symmetrical cross section, with the eventual load eccentricity along the symmetry axes, due to the lack of other cases experimentally considered. Rotation φ_i between the principal gross and effective axis is hence zero (i.e., $\varphi_i=0$), i.e., the two reference systems are translated and not rotated;
- the values of the elastic section moduli of the effective cross section, $W_{e,u,i}$ and $W_{e,v,i}$, in the principal axes of the effective section;
- the value of the limit load multiplier α_i^*;

Furthermore, the ratio between the experimental ultimate load N_{exp} and the axial predicted load carrying capacity $\alpha_R \cdot N$ is reported.

4.1 APPLICATION TO COLD-FORMED ANGLES

In 1999, Popovic, Hancock and Rasmussen [12] investigated the behaviour of cold-formed angles. Reference was done to an equal edge angle with 50 mm long legs, for which three different thicknesses (2.5 mm, 4 mm and 5 mm) were considered. In total 36 specimens were tested, differing in specimen length as well as in the value of the load eccentricity. In the following, the present approach is used to predict the load carrying capacity of the thinner cross-section (fig. 7a) of the specimens listed below:

- LO24041 (L50x50x2.5): the specimen has a slenderness $\lambda = 20.12$ and it is subjected to axial load. The experimental load carrying capacity is 54,0 kN;

• LO24101 (L50x50x2.5): the specimen has a slenderness λ = *49.50* and it is subjected to axial load. The experimental load carrying capacity is 37,0 kN;

• LP24192 (L50x50x2.5): the specimens has a slenderness λ = *112.27* and it is subjected to eccentric axial load with a small eccentricity. The experimental load carrying capacity is 24.7 kN.

In table 1, the main results of the approach applied to angle specimens are summarised. Independently of the accuracy of the approach, which will be discussed in the companion paper [9], it should be noted that convergence requires only a few iterations for a specimen with a small or medium value of slenderness. When the longer specimen is considered, the number of iterations increases significantly as it results by the value of the load multiplier α_3^*, which is very near to α_{13}^* ($=\alpha_R$), while α_3 is very different from α_3^*. The resistant section is coincident with the gross-section (i.e., at the end of the iterative procedure, the section is fully effective). Furthermore, it should be noted that increasing the value of the specimen slenderness, the value of the form factor increases, to the limit of 1. This slow convergence for high slenderness values is due to the need for recovering gross-section properties, starting from the partially effective section of iteration 1. In the present approach a bisection method is used (see §2.7). A much better convergence could be achieved by using a Newton-like iterative scheme, but this improvement was outside the scope of the present work.

Figure 8 presents the effective sections for the considered angle specimens, which differ for the leg length. It has to be pointed out that, despite loss of area is quite moderate, being not greater than 14%, effective section second moment of area and section moduli are significantly reduced (up to 36% and 27%, respectively), with reference to the properties evaluated on the gross-section.

4.2 APPLICATION TO LIPPED CHANNELS

Young and Rasmussen [13] carried out a study on the load carrying capacity of cold-formed lipped channels by testing two geometries of cross section and different specimen lengths. Herein, reference is done to the cross section presented in figure 7b) and the load carrying capacity is predicted for the following specimens under axial load:

• specimen L36F0280: the specimen has a slenderness $\lambda = 10.18$ and the experimental load carrying capacity is 100.2 kN;

• specimen L36F1500: the specimen has a slenderness $\lambda = 54.54$ and the experimental load carrying capacity is 82.4 kN;

• specimen L36F3000: the specimen has a slenderness $\lambda = 108.96$ and the experimental load carrying capacity is 39.3 kN.

In table 2, the main results of the approach applied to lipped channel specimens are summarised.

As to the convergence, general remarks done for the angle cases are confirmed for lipped as well as for other types of thin walled members. The effective section does not coincide with the gross-section and the ineffective zones are presented in figures 9 and 10 for the cases of shorter (L36F280) and longer (L36F3000) specimen. It should be noted that, despite the high value of slenderness of specimen L36F3000 (λ = 108.96), the gross-section is not fully effective (Q=0.968).

In case of shorter specimens, despite that loss of area is approximately 17% of the gross-area, reduction of second moment of area as well as section moduli is more limited (respectively not greater than 13% and 4%), due to the different position of loss area. While for angles the loss area is at the end of the legs, for lipped channels it is distributed across the web centre.

Figures 9 and 10 report gross-section and effective cross-section

	Specimen (effective length)								
	LO24041 (λ = 20.12)			*LO24101 (λ = 49.50)*			*LO24192 (λ = 112.27)*		
iteration	*i=1*	*i=2*	*i=4*	*i=1*	*i=3*	*i=5*	*i=1*	*i=3*	*i=13*
α_i	*91291*	*56084*	*46615*	*91291*	*37691*	*37516*	*73711*	*29497*	*18987*
$Q_i = \frac{A_{ei}}{A_g}$	*0.674*	*0.807*	*0.861*	*0.674*	*0.926*	*0.928*	*0.765*	*1.000*	*1.000*
$I_{e,u,i}$ [mm⁴]	*29095*	*49433*	*59949*	*29095*	*74244*	*74584*	*42318*	*93022*	*93022*
$I_{e,v,i}$ [mm⁴]	*6753*	*11619*	*14147*	*6753*	*17592*	*17675*	*9912*	*22131*	*22131*
$W_{e,u,i}$ [mm³]	*1198.4*	*1715.9*	*1954.9*	*1198.4*	*2258.7*	*2265.7*	*1545.3*	*2631.1*	*2631.1*
$W_{e,v,i}$ [mm³]	*549.9*	*798.6*	*914.0*	*549.9*	*1061.0*	*1064.3*	*716.8*	*1242.1*	*1242.1*
α_i^*	*20877*	*37061*	*46604*	*11483*	*37221*	*37485*	*8205*	*18977*	*18977*
$\frac{N_{exp}}{\alpha_R \cdot N}$			*1.159*			*0.987*			*1.302*

Table 1: key data of the unified approach applied to equal angle specimens

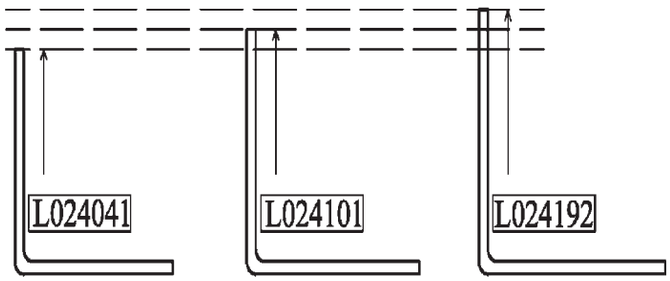

Figure 8: effective section for the considered angle specimens

for intermediate as well as last iteration for the shorter and longer specimens, respectively.

5 COMPARISONS WITH EXISTING STANDARDS

The method herein proposed is different from Eurocode 3 part 1-3 for these main reasons:

- resistance and stability checks are done at the same time, i.e. there is no need to perform a resistance check independent of overall stability check;
- axial force and bending moments define a unique effective cross section, there are not three different cross sections that are independent from each other;
- overall stability is here performed using effective cross section properties associated with the externally applied loads, while Eurocode 3 part 1-3 uses an hydrid formula which uses gross-section second area moment and effective section area to compute radius of inertia to be used in slenderness definition formula;
- in the proposed method, changes in load levels do affect effective section, while the effective section area and bending moduli used by Eurocode 3 part 1-3 are computed irrespective to the applied load level.

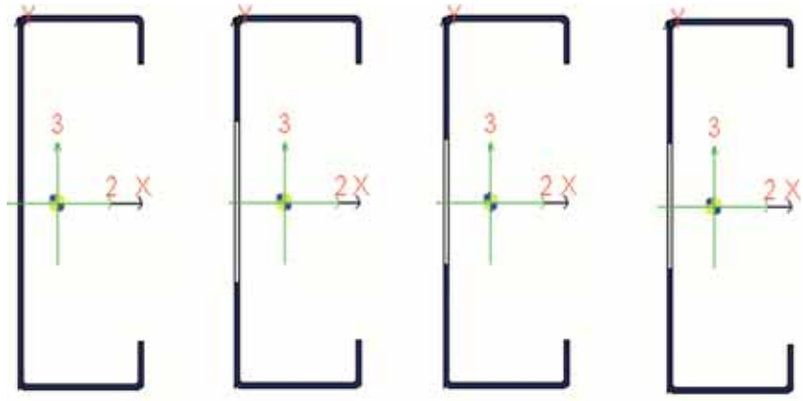

Initial cross-section | *Effective cross-section at 1st iteration* | *Effective cross-section at 4th iteration* | *Effective cross-section at the final (8th) iteration*

Figure 9: evolution of the effective cross-section for L36F0280 specimen

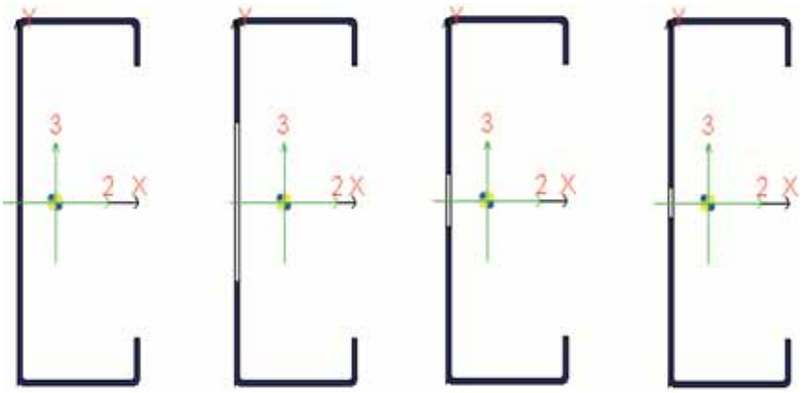

Initial cross-section | *Effective cross-section at 1st iteration* | *Effective cross-section at 4th iteration* | *Effective cross-section at the final (10th) iteration*

Figure 10: evolution of the effective cross-section for L36F3000 specimen

	Specimen (effective length)								
	L36F0280 (λ = 10.18)			*L36F1500 (λ = 54.54)*			*L36F3000 (λ = 108.96)*		
iteration	*i=1*	*i=4*	*i=8*	*i=1*	*i=4*	*i=9*	*i=1*	*i=6*	*i=10*
a_i	146741	97758	95279	146124	74930	70780	146202	37256	36093
$Q_i = \frac{A_{e,i}}{A_g}$	0.774	0.823	0.826	0.772	0.854	0.862	0.773	0.951	0.968
$I_{e,u,i}$ [mm⁴]	402881	407831	408082	402496	409776	410160	401959	411666	411690
$I_{e,v,i}$ [mm⁴]	43858	46434	46596	43665	47873	48223	43800	52067	52233
$W_{e,u,i}$ [mm³]	8281.2	8383.0	8388.1	8256.3	8405.7	8413.5	8253.8	8453.1	8453.6
$W_{e,v,i}$ [mm³]	1978.8	2019.5	2021.9	1975.1	2040.2	2045.3	1983.9	2105.1	2107.3
a_i^*	83489	94459	95233	56700	69484	70754	25336	35746	36067
$\frac{N_{exp}}{a_R \cdot N}$			1.052			1.165			1.090

Table 2: key data of the unified approach applied to lipped channel specimens

The method here proposed is different from AISI direct strength method (DSM) at least for the following reasons:

• DSM distinguishes between resistance and stability checks, while the method here presented does not;

• DSM "provides no explicit provisions for members under combined axial load and bending (beam-columns)" ([5], appendix 1);

• no finite element/strip method has to be used in the present approach, while this is needed using DSM;

• in DSM overall member buckling load is computed using gross section properties while in the method here presented effective section properties are taken into account, as well as in resistance checks, so the member actually considered is always the effective one, and there is no mixed use of gross vs effective properties in the prediction of load carrying capacity.

6 CONCLUSIONS

The prediction of the load carrying capacity of thin-walled cold-formed steel members under constant axial eccentric load has been considered in this paper. The proposed method defines the effective section directly on the basis of stress levels acting on members. This prediction method, which is based on an iterative procedure, can be used for practical design since its degree of accuracy has been proven during the phase based on experimental results. The Authors believe that one of the best features of the proposed method is its formal clearness since it avoids the use of ad hoc formulations. Furthermore, the unified approach is quite simple to understand, being based on very clear key concepts that are: 1) effective section depends strictly on the load level and 2) effective member buckles just depending on its effective section properties, with no memory of its gross-section original features.

As to the method assumptions, it should be pointed out that:

• a constant stress distribution, and therefore a constant effective section along the member axis has been considered, so that an "effective member", that is a member with constant effective section, can be clearly defined and used for design. For more generic load conditions on a member (i.e. variable moments), the change of effective section along member axis is quite a complex problem, also for more traditional steel members, which has traditionally been "solved" by using distribution factors to be applied to maximum bending moments. This problem is currently under investigation by the Authors;

• distortional failure modes have not yet been considered;

• a key point in setting up the method (and a possible source of further investigations) are the interaction formulae used to compute the effective member's load carrying capacity. Alternative interaction formulae can possibly provide better results (e.g. Eurocode 3-part1-1 [15] method 2, for instance);

• further improvements of the algorithm can be obtained by changing it into a Newton-like root finder, that is using derivatives of a, however such investigation was beyond the scope of this work.

An appraisal of the degree of accuracy of the proposed method is available in the companion paper [9], where 229 tests have been simulated, showing that the overall average percentage error of the estimated load carrying capacity versus the experimental one is lower than 4%.

***Prof. dr. ing. Claudio Bernuzzi**, Department of Structural Engineering, Politecnico di Milano, Milano (I)*

***Dr. ing. Paolo Rugarli**, Structural Engineer, Castalia s.r.l., Milano (I)*

REFERENCES

[1] Rodhes J., Design of cold formed steel members, Elsevier Applied Science, 1991.

[2] Ghersi A., Landolfo R., Mazzolani F.M., Design of metallic Cold-formed thin-walled members, Spon Press, 2002.

[3] CEN, ENV 1993-1-3:1996: Eurocode 3: Design of steel structures, Part 1.3: General rules-Supplementary rules for cold-formed thin gauge members and sheeting, European Committee for Standardisation.

[4] CEN, pr EN 1993-1-3:2005: Eurocode 3: Design of steel structures, Part 1-3: General rules-Supplementary rules for cold-formed members and sheeting, (Draft February 2006) European Committee for Standardisation.

[5] AISI, Cold formed steel design manual, American Iron and Steel Institute, 2004 edition.

[6] Von Karman T., Sechler E.E., Donnel L.H., The strength of thin plates in compression, Transactions A.S.M.E., APM-54-5, , Vol. 54, 1932, pp. 53-57.

[7] Winter G., Strength of thin steel compression flanges, Transactions A.S.C.E., paper n. 2305, February 1946, pp. 527-576.

[8] CEN, pr EN 1993-1-5:2006: Eurocode 3: Design of steel structures, Part 1-5: Plated structural elements, (Draft February 2006) European Committee for Standardisation.

[9] Bernuzzi C., Rugarli P. An approach for the prediction of the load carrying capacity of slender cross-section members under Eccentric Axial Load. Part 2:Validation, 2008, submitted to Costruzioni Metalliche for publication.

[10] Rugarli P., Elastic and plastic flexural properties: computerised calculation of generic sections, (in Italian) Costruzioni Metalliche 4/1998

[11] Castalia srl: "Sargon©" user's manual.

[12] Popovic, G.J. Hancock and K.J. Rasmussen, Axial compression tests of cold formed angles, ASCE Journal of Structural Engineering, May 1999, pp. 515-523.

[13] Young B. and Rasmussen J.R., Tests of fixed–ended plain channel columns, Journal of Structural Engineering, vol. 124, nr. 2, May 1998, pp. 131 - 139.

[14] Young B. and Rasmussen J.R., Behaviour of cold formed singly symmetric columns, Thin-walled Structures, vol. 33,1999, pp. 83 – 102.

[15] EN 1993-1-1 Eurocode 3 part 1-1 "Design of steel structures – General rules and rules for buildings".

ACKNOWLEDGEMENTS

The approach has been implemented in a computer programme by the software house Castalia s.r.l. (www.castaliaweb.com), to which the Authors would sincerely like to express their thanks.

Appendix A: Notation

The meaning of each symbol used in the paper is generally explained when it appears first in the text. However, for convenience, symbols are listed below.

Symbols:

A	area
b	width of the wall
f	tension, stress
E	Young modulus
Err	error
G	cross-section centroid
I	second moment of area
N	axial load
M	bending moment
P	generic point of the cross-section
Q	form factor
S	vectorial notation for applied load
t	thickness of the wall
Tol	tolerance
W	section modulus
X	principal axis for gross-section
Y	principal axis for gross-section

Greek letters:

α	load multiplier
β	effective length factor
ρ	radius of inertia
β	slenderness factor
ΔM	additional moment
φ	angle between the principal axes of gross-section and the ones of effective section
λ	slenderness
ψ	stress ratio
ν	Poisson ratio
ρ	reduction factor
σ	tension
Ω	section domain

Index:

c	compression
com	maximum value
cr	critical
d	design
e	effective, elastic
eff	effective
exp	experimental
$e1$	effective at extreme 1
$e2$	effective at extreme 2
f	flexural
ft	flexural-torsional
g	gross
i	iteration index
lim	limit
p	relative
pl	plastic
red	reduced
R	load carrying capacity
T	tension
T	total
u	principal axis for effective section
v	principal axis for effective section
y	yield, principal axis for gross-section
x	principal axis for gross-section
1	extreme of the plate element
2	extreme of the plate element

Special symbols:

α_i^*	member load multiplier in current iteration
k_σ	local buckling coefficient
$\overline{\lambda}$	non dimensional slenderness

Appendix B: By hand prediction of the load carrying capacity of hollow square column

The column has an effective length of 4000 mm (fig. A1a) and its cross section is a hollow square tube 200x200 having a thickness of 4 mm (figure A1b). For the sake of simplicity sharp corners have been assumed. Yield tension f_y is 355 N / mm^2, Young modulus E is 210000 N / mm^2 and Poisson ratio (v) is 0.3.

Main properties of the tube gross section are:

- Area = A_g = 3136 mm^2
- Second moment of area = I_g = 20087125 mm^4

Reference for hand computation is made to the middle line of the cross-section, i.e., by considering the profile composed by plates 196 mm width. The value of the axial load is 10000 N and tol=0.01 is assumed as limit for tolerance.

Evaluation of the critical elastic buckling stress.

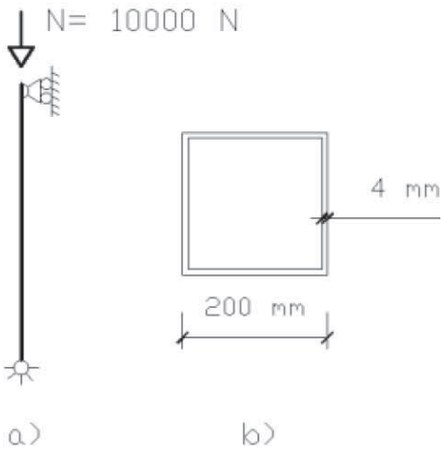

Figure A1

Due to the shape of the cross section of member, buckling coefficient $k\sigma$ assumes the value of 4.

eq. 4)

$$\sigma_{cr} = k_\sigma \cdot \frac{\pi^2 E}{12\cdot(1-\upsilon^2)} \cdot \left(\frac{t}{b}\right)^2 = 4 \cdot \frac{\pi^2 \cdot 210000}{12\cdot(1-0.3^2)} \cdot \left(\frac{4}{196}\right)^2 = 316.202 \ N/mm^2$$

Iteration 1

• Step 1: Initialization of load multiplier (§ 2.1)

eq. 6)

$$\alpha_1 \left(\frac{N}{N_{lim}}\right) = \alpha_1 \left(\frac{N}{A_g \cdot f_y}\right) = \alpha_1 \left(\frac{10000}{3136\cdot 355}\right) = 1$$

$$\alpha_1 = 111.328$$

• Step 2: Stress computation and assessment of the effective width (§ 2.2)

Stresses are constant across the section. In case of first iteration they correspond to the yielding tension f_y, i.e.:

eq. 7)

$$\sigma_1 = \frac{\alpha_1 N}{A_g} = \frac{111.328\cdot 10000}{3136} = 355 \ N/mm^2$$

Assessment of effective width

eq. 5)

$$\bar{\lambda}_{p,1} = \sqrt{\frac{\sigma_1}{\sigma_{cr}}} = \sqrt{\frac{355}{316.202}} = 1.0596$$

eq. 3a)

$$b_{e,1} = \frac{1}{\bar{\lambda}_{p,1}} \cdot \left[1 - 0.055 \cdot (3+\psi) \cdot \frac{1}{\bar{\lambda}_{p,1}}\right] \cdot b =$$

$$= \frac{1}{1.0596} \cdot \left[1 - 0.055 \cdot (3+1) \cdot \frac{1}{1.0596}\right] \cdot 196 = 0.7478 \cdot 196 = 146.572 \ mm$$

• Step 3: Computation of effective section properties (§ 2.3)

$$A_{e,1} = 4 \cdot b_{e,1} \cdot t = 4 \cdot (146.572 \cdot 4) = 2345.2 \ \ mm^2$$

$$b_{p,1} = b - b_{e,1} = 196 - 146.572 = 49.428 \ \ mm$$

$$I_{e,1} = I_g - 2 \cdot \left[\frac{b_{p,1} \cdot t^3}{12} + (b_{p,1} \cdot t) \cdot \left(\frac{b}{2}\right)^2\right] - 2 \cdot \frac{b_{p,1}{}^3 \cdot t}{12} =$$

$$= 20087125 - 2 \cdot \left[\frac{49.428 \cdot 4^3}{12} + (49.428 \cdot 4) \cdot \left(\frac{196}{2}\right)^2\right] - 2 \cdot \frac{49.428^3 \cdot 4}{12} = 16208465 \ mm^4$$

Effective ratius of gyration $\rho_e 1$

$$\rho_{e,1} = \sqrt{\frac{I_{e,1}}{A_{e,1}}} = \sqrt{\frac{16208465}{2345.1}} = 83.135 \ \ mm$$

• Step 4: Computation of the loads on effective section (§ 2.4)

In this case, due to the presence of two axis of symmetry, no shift of centroid and no rotation of principal axis occur, i.e., in accordance with eqs 8):

$$N = 10000 \ N$$

$$\Delta M_x = 0$$

$$\Delta M_y = 0$$

Owing to the shape of the cross-section and to the presence of pure compression, this step is omitted in the following iterations.

• Step 5: Evaluation of the load multiplier α_1* (§ 2.4)

Limit axial strength, in accordance with EC3 criteria for check of stability of compressed member, is given by:

$$N_{c,1,lim} = \chi_1 \cdot A_{e,1} \cdot f_y$$

Reduction factor χ is given by:

$$\chi_1 = \frac{1}{\varphi_1 + \sqrt{\varphi_1^2 - \bar{\lambda}_1^2}} = \frac{1}{0.7713 + \sqrt{0.7713^2 - 0.6297^2}} = 0.8219$$

Terms $\bar{\lambda}_1$ and φ_1 assume the values:

$$\bar{\lambda}_1 = \frac{\lambda_1}{\lambda_p} = \frac{l_0/\rho_{e,1}}{\pi\sqrt{\frac{E}{f_y}}} = \frac{4.000/83.135}{\pi\sqrt{\frac{210.000}{355}}} = \frac{48.114}{76.409} = 0.6297$$

$$\varphi_1 = 0.5 \cdot [1 + \alpha(\bar{\lambda}_1 - 0.2) + \bar{\lambda}_1^2] = 0.5 \cdot [1 + 0.34 \cdot (0.6297 - 0.2) + 0.6297^2] = 0.7713$$

The value of the limit axial load on the effective section at the first iteration is:

$$N_{c,1,lim} = 0.8219 \cdot 2345.1 \cdot 355 = 684240 \ N$$

Term α_1* is obtained as:

eq. 13)

$$\alpha_1^* = \frac{N_{c,1,lim}}{N} = \frac{684240}{10000} = 68.424$$

• Step 6: Check for tolerance (§ 2.6)

eq.18)

$$Err_1 = \frac{|\alpha_1^* - \alpha_1|}{\alpha_1} = \frac{|68.424 - 111.328|}{111.328} = 0.385$$

being this value greater than limit of tolerance (toll=0.01) a new iteration is necessary.

• Step 7: Correction and new iteration (§ 2.7)

Eq. 19)

$$\alpha_2 = \frac{\alpha_1 + \alpha_1^*}{2} = \frac{111.328 + 68.424}{2} = 89.876$$

Iteration 2

• Step 2: Stress computation and assessment of the effective width (§ 2.2)

Stress computation

eq. 7)

$$\sigma_2 = \frac{a_2 N}{A_g} = \frac{89.876 \cdot 10.000}{3136} = 286.59 \ N/mm^2$$

Being $\sigma < f_y$ reduced non dimentional slenderness $\bar{\lambda}_{p,red}$ has to be used in eqs 3a)

Reduced non dimensional slenderness:

eq. 5)

$$\bar{\lambda}_{p,2} = \sqrt{\frac{\sigma_2}{\sigma_{cr}}} = \sqrt{\frac{286.59}{316.202}} = 0.9520$$

Assessment of effective width (§ 2.2)

eq.3a)

$$b_{e,2} = \frac{1}{\bar{\lambda}_{p,2}} \cdot \left[1 - 0.055 \cdot (3+\psi) \cdot \frac{1}{\bar{\lambda}_{p,2}}\right] \cdot b =$$

$$= \frac{1}{0.952} \cdot \left[1 - 0.055 \cdot (3+1) \cdot \frac{1}{0.952}\right] \cdot 196 = 0.8077 \cdot 196 = 158.301 \ mm$$

• Step 3: Computation of effective section properties (§ 2.3)

$A_{e,2} = 4 \cdot b_{e,2} \cdot t = 4 \cdot 158.301 \cdot 4 = 2532.8 \ \ mm^2$

$b_{p,2} = b - b_{e,2} = 196 - 158.301 = 37.699 \ \ mm$

$$I_{e,2} = I_g - 2 \cdot \left[\frac{b_{p,2} \cdot t^3}{12} + b_{p,2} \cdot t \cdot \left(\frac{b}{2}\right)^2\right] - 2 \cdot \frac{b_{p,2}{}^3 \cdot t}{12} =$$

$$= 20087125 - 2 \cdot \left[\frac{37.699 \cdot 4^3}{12} + 37.699 \cdot 4 \cdot \left(\frac{196}{2}\right)^2\right] - 2 \cdot \frac{37.699^3 \cdot 4}{12} = 17154494 \ \ mm^4$$

Effective ratius of gyration $\rho_{e,2}$

$$\rho_{e,2} = \sqrt{\frac{I_{e,2}}{A_{e,2}}} = \sqrt{\frac{17154494}{2532.8}} = 82.298 \ mm$$

• Step 5: Evaluation of the load multiplier a_2* (§ 2.4)

Limit axial strength is given by:

$N_{c,2,lim} = \chi_2 \cdot A_{e,2} \cdot f_y$

$$\chi_2 = \frac{1}{\varphi_2 + \sqrt{\varphi_2{}^2 - \bar{\lambda}_2{}^2}} = \frac{1}{0.7765 + \sqrt{0.7765^2 - 0.6361^2}} = 0.8185$$

being $\bar{\lambda}_2$ terms and φ_2 defined as:

$$\bar{\lambda}_2 = \frac{\lambda_2}{\lambda_p} = \frac{l_0/\rho_{e,2}}{\pi\sqrt{\frac{E}{f_y}}} = \frac{4000/82.298}{\pi\sqrt{\frac{210000}{355}}} = \frac{48.604}{76.409} = 0.6361$$

$$\varphi_2 = 0.5 \cdot [1 + \alpha(\bar{\lambda}_2 - 0.2) + \bar{\lambda}_2{}^2] = 0.5 \cdot [1 + 0.34 \cdot (0.6361 - 0.2) + 0.6361^2] = 0.7765$$

The value of the limit axial load on the effective section is:

$N_{c,2,lim} = 0.8185 \cdot 2532.8 \cdot 355 = 735980 \ N$

Term a_2* is obtained as

eq. 13)

$$a_2^* = \frac{N_{c,2,lim}}{N} = \frac{735980}{10000} = 73.598$$

• Step 6: Check for tolerance (§ 2.6)

eq.18)

$$Err_2 = \frac{|a_2^* - a_2|}{a_2} = \frac{|73.598 - 89.876|}{89.876} = 0.181 > 0.01 (= tol)$$

• Step 7: Correction and new iteration (§ 2.7)

eq. 19)

$$a_3 = \frac{a_2 + a_2^*}{2} = \frac{89.876 + 73.596}{2} = 81.737$$

Iteration 3

• Step 2: Stress computation and assessment of the effective width (§ 2.2)

eq. 7)

$\sigma_3 = \frac{a_3 N}{A_g} = 260.641 \ N/mm^2 < f_y$

eq. 5)

$$\bar{\lambda}_{p,3} = \sqrt{\frac{\sigma_3}{\sigma_{cr}}} = 0.9079$$

eq. 3a)

$$b_{e,3} = \frac{1}{\bar{\lambda}_{p,3}} \cdot \left[1 - 0.055 \cdot (3+\psi) \cdot \frac{1}{\bar{\lambda}_{p,3}}\right] \cdot b = 163.570 \ mm$$

• Step 3: Computation of effective section properties (§ 2.3)

$A_{e,3} = 4 \cdot b_{e,3} \cdot t = 2617.1 \ \ mm^2$

$b_{p,3} = b - b_{e,3} = 32.430 \ \ mm$

$$I_{e,3} = I_g - 2 \cdot \left[\frac{b_{p,3} \cdot t^3}{12} + b_{p,3} \cdot t \cdot \left(\frac{b}{2}\right)^2\right] - 2 \cdot \frac{b_{p,3}{}^3 \cdot t}{12} = 17572407 \ \ mm^4$$

$$\rho_{e,3} = \sqrt{\frac{I_{e,3}}{A_{e,3}}} = 81.941 \ mm$$

• Step 5: Evaluation of the load multiplier a_3* (§ 2.4)

$N_{c,3,lim} = \chi_3 \cdot A_{e,3} \cdot f_y = 759129 \ N$

$$\chi_3 = \frac{1}{\varphi_3 + \sqrt{\varphi_3{}^2 - \bar{\lambda}_3{}^2}} = \frac{1}{0.7787 + \sqrt{0.7787^2 - 0.6389^2}} = 0.8171$$

eq. 13)

$$a_3^* = \frac{N_{c,3,lim}}{N} = \frac{759122}{10000} = 75.913$$

• Step 6: Check for tolerance (§ 2.6)
eq.18)

$$Err_3 = \frac{|a_3^* - a_3|}{a_3} = 0.071 > 0.01 (= tol)$$

• Step 7: Correction and new iteration (§ 2.7)
eq. 19)

$$a_4 = \frac{a_3 + a_3^*}{2} = 78.825$$

Iteration 4
• Step 2: Stress computation and assessment of the effective width (§ 2.2)
eq. 7)

$$\sigma_4 = \frac{a_4 N}{A_g} = 251.355 \ N/mm^2 < f_y$$

eq. 5)

$$\bar{\lambda}_{p,4} = \sqrt{\frac{\sigma_4}{\sigma_{cr}}} = 0.8916$$

eq. 3a)

$$b_{e,4} = \frac{1}{\bar{\lambda}_{p,4}} \cdot \left[1 - 0.055 \cdot (3 + \psi) \cdot \frac{1}{\bar{\lambda}_{p,4}} \right] \cdot b = 165.589 \ mm$$

• Step 3: Computation of effective section properties (§ 2.3)

$$A_{e,4} = 4 \cdot b_{e,4} \cdot t = 2649.4 \ \ mm^2$$
$$b_{p,4} = b - b_{e,4} = 30.411 \ \ mm$$

$$I_{e,4} = I_g - 2 \cdot \left[\frac{b_{p,4} \cdot t^3}{12} + b_{p,4} \cdot t \cdot \left(\frac{b}{2} \right)^2 \right] - 2 \cdot \frac{b_{p,4}^3 \cdot t}{12} = \ 17731537 \ \ mm^4$$

$$\rho_{e,4} = \sqrt{\frac{I_{e,4}}{A_{e,4}}} = 81.808 \ mm$$

• Step 5: Evaluation of the load multiplier a_4* (§ 2.4)

$$N_{c,4,lim} = \chi_4 \cdot A_{e,4} \cdot f_y = 767984 \ N$$

$$\chi_4 = \frac{1}{\varphi_4 + \sqrt{\varphi_4^2 - \bar{\lambda}_4^2}} = \frac{1}{0.7795 + \sqrt{0.7795^2 - 0.6399^2}} = 0.8165$$

eq. 13)

$$a_4^* = \frac{N_{c,4,lim}}{N} = \frac{767984}{10000} = 76.798$$

• Step 6: Check for tolerance (§ 2.6)
eq.18)

$$Err_4 = \frac{|a_4^* - a_4|}{a_4} = 0.0257 > tol (= 0.01)$$

• Step 7: Correction and new iteration (§ 2.7)
eq. 19)

$$a_5 = \frac{a_4 + a_4^*}{2} = 77.812$$

Iteration 5
• Step 2: Stress computation and assessment of the effective width (§ 2.2)
eq. 7)

$$\sigma_5 = \frac{a_5 N}{A_g} = 248.124 \ N/mm^2 < f_y$$

eq. 5)

$$\bar{\lambda}_{p,5} = \sqrt{\frac{\sigma_5}{\sigma_{cr}}} = 0.8858$$

eq.3a)

$$b_{e,5} = \frac{1}{\bar{\lambda}_{p,5}} \cdot \left[1 - 0.055 \cdot (3 + \psi) \cdot \frac{1}{\bar{\lambda}_{p,5}} \right] \cdot b = 166.310 \ mm$$

• Step 3: Computation of effective section properties (§ 2.3)

$$A_{e,5} = 4 \cdot b_{e,5} \cdot t = 2661.0 \ \ mm^2$$

$$b_{p,5} = b - b_{e,5} = 29.690 \ \ mm$$

$$I_{e,5} = I_g - 2 \cdot \left[\frac{b_{p,5} \cdot t^3}{12} + b_{p,5} \cdot t \cdot \left(\frac{b}{2} \right)^2 \right] - 2 \cdot \frac{b_{p,5}^3 \cdot t}{12} = \ 17788192 \ \ mm^4$$

$$\rho_{e,5} = \sqrt{\frac{I_{e,5}}{A_{e,5}}} = 81.761 \ mm$$

• Step 5: Evaluation of the load multiplier a_5* (§ 2.4)

$$N_{c,5,lim} = \chi_5 \cdot A_{e,5} \cdot f_y = 771141 \ N$$

$$\chi_5 = \frac{1}{\varphi_5 + \sqrt{\varphi_5^2 - \bar{\lambda}_5^2}} = \frac{1}{0.7798 + \sqrt{0.7798^2 - 0.6403^2}} = 0.8163$$

eq. 13)

$$a_5^* = \frac{N_{c,5,lim}}{N} = \frac{771141}{10000} = 77.114$$

• Step 6: Check for tolerance (§ 2.6)
eq.18)

$$Err_5 = \frac{|a_5^* - a_5|}{a_5} = 0.0090 < 0.01 (= tol)$$

Load multiplier leading member to achieve its load carrying capacity is $a_R = a_5 = 77.114$